IEEE Access
Multidisciplinary | Rapid Review | Open Access Journal

Received March 7, 2020, accepted April 14, 2020, date of publication April 28, 2020, date of current version May 7, 2020.

Digital Object Identifier 10.1109/ACCESS.2020.2990906

Method of Four-Element Retrodirective Cross-Eye Jamming Based on DoA

WEI LIU, JIN MENG, AND LIANG ZHOU
National Key Laboratory of Science and Technology on Vessel Integrated Power System, Naval University of Engineering, Wuhan 430033, China
Corresponding author: Liang Zhou (zhou201314l@163.com)

ABSTRACT The cross-eye method is commonly used to interfere monopulse radars. To overcome the strict tolerance and the range limitation of the traditional retrodirective cross-eye method and the multi-loop method, a novel four-element retrodirective cross-eye based on Direction of Arrival (DoA) is proposed. The mathematical model of the four-element retrodirective cross-eye jamming is derived based on the method of expansibility analysis, and the general formulas of indication angle are obtained. Based on the DoA information, the antenna layout of jamming loops is optimized, and the influence of the modulation parameters on cross-eye jamming effect are analyzed. The orthogonal four-element retrodirective cross-eye is compared with the traditional cross eye jamming, the results show that the the proposed method is superior to the traditional and the orthogonal four-element retrodirective cross-eye in terms of the jamming effect and the modulation parameter tolerance.

INDEX TERMS Cross-eye, monopulse radar, direction of Arrival (DoA), modulation parameters.

I. INTRODUCTION

Monopulse radar is widely used in precision-guided weapons [1], [2] because of its ability of precise angle measurement and strong anti-jamming characteristic. Therefore, in order to protect the aircrafts, ships and other combat platforms from attack of the precision-guided weapons, effective jamming of monopulse radar has been a research hotspot in the field of electronic warfare [3], [4].

The cross-eye jamming method is proposed based on the angle glint phenomenon [5], which is one of the most effective ways to jam monopulse radar. By transmitting two signals with similar amplitude and opposite phase, the jamming source makes the monopulse radar point deviate from the target position [6]. In the early stage, two independent jamming sources were used. However, this method cannot be directly used in engineering, due to the poor controllability of the amplitude and the phase of the two jamming signals [7]. The reverse antenna structure [8], [9] was introduced into the cross-eye jamming, by Plessis, a South African scholar, who carried out the strict mathematical analysis and the experimental verification on the two-element cross-eye jamming model [10]–[13]. By modeling the sum difference channel of the monopulse radar, Liu concluded that the cross-eye jamming would cause the distortion of the difference channel pattern, and then affect the radar angle measurement [14]. The power design of the cross-eye jammer based on the linear fitting method is analyzed in reference [15]. The[1] research above mainly focuses on the two-element retrodirective cross-eye jamming. To overcome the shortcomings of the two-element retrodirective cross-eye jamming in terms of the interference performance and the parameter tolerance, the multi-element retrodirective cross-eye is proposed. Liu put forward the orthogonal multi-element retrodirective cross-eye jamming model to solve the problem of deception angle instability caused by the change of jamming platform and radar position, and made a quantitative analysis of its parameter tolerance and angle deception stability by deception??? angle stability factor [16], [17]. But they did not consider that they should be applied to the case where the baseline length of two jamming loops is different under different platform conditions; Liu considered the platform echo, modeled the multi-element linear array reverse cross-eye jamming, and pointed out that under the same deception angle, its parameter tolerance was more relaxed than the traditional cross-eye model [18], [19]. In reference [20], the requirement of interference to signal ratio of cross- eye is analyzed by using the median gain of cross-eye.

The associate editor coordinating the review of this manuscript and approving it for publication was Guolong Cui.

[1]This work was supported in part by National Natural Science Foundation of China (71801220, 61801502)

The conditions for stable interference are also pointed out. In reference [21], for the strict parameter tolerance and limitation of action range of two-element retrodirective cross-eye, the retrodirective cross-eye of rectangular array is introduced, and guided by the optimal layout factor. Different layout models of the rectangular array are carried out. The research mentioned above on multi-element mainly focuses on the way of regular shape comparison such as the linear array and the orthogonal layout, but the cross-eye jamming model of arbitrary layout is not studied. In this paper, the research object is the retrodirective cross-eye jamming system which is distributed on the target platform. Considering the limitation of the application of multiple-point source retrodirective cross-eye on different platforms, a general model of four-element retrodirective cross-eye is proposed. According to the angle measurement principle of monopulse radar, the indication angle of monopulse radar is deduced, and the DoA information [22] is introduced for analysis. The influence of the jamming loop antenna distribution on the jamming effect of the cross-eye is discussed, and the optimal distribution model of the interference antenna is obtained. Finally, the traditional two-element cross-eye jamming model and the orthogonal four-element retrodirective cross-eye model are compared with the proposed model in terms of the modulation parameter freedom and the jamming effect under the same conditions. The simulation results can provide guidance for the layout design of the cross-eye jamming.

II. FOUR-ELEMENT RETRODIRECTIVE CROSS-EYE JAMMING MODEL BASED ON DoA

The proposed model is composed of two groups of jamming loops, each of which adopts the reverse antenna structure of single receiving and transmitting antenna [23], [24], as shown in Fig. 1. The signal transmission between the antenna pairs is mainly based on the digital store and the forward technology [25]. The specific process is as follows: The signal of the monopulse radar will be received by antenna 1 and antenna 2. The received signal of antenna 2 is transmitted to antenna 1 after power amplification through baseline, and then transmitted to the direction of radar by antenna 1. The amplitude and phase of the received signal of antenna 1 will be modulated and transmitted to antenna 2, and then transmitted by antenna 2 to the direction of radar. For the convenience of description, the modulation direction of the jamming loops is defined as: antenna 1 to antenna 2. Because the reverse antenna structure shares the signal receiving, the transmitting antennas, and the transmission feeders,the phase difference and the power loss difference are ignored.

The position distribution of the jammer and the monopulse radar is shown in Fig. 2. Two dots on the left represent the antennas of the monopulse radar. Four dots on the right represent the cross-eye jamming system which is composed of two jamming loops. It is assumed that the jamming system is distributed on the target platform, and the center of the target platform coincides with the center of the jamming system. Antenna 1 and antenna 2 form a group of reverse

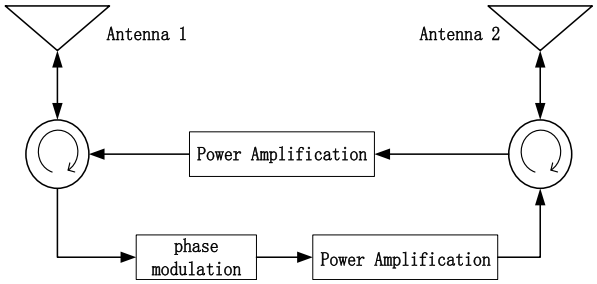

FIGURE 1. Antenna structure of retrodirective cross-eye.

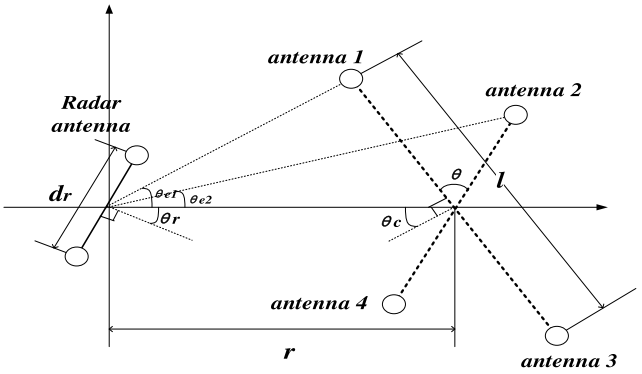

FIGURE 2. Position distribution of jammer and monopulse radar.

antenna pairs, which are called the jamming loop 1. They are connected by baseline. Antenna 3 and antenna 4 form another group of reverse antenna pairs, which are defined as the jamming loop 2. The centers of the two jamming loops coincide. The line between the center of radar antennas and the center of jamming system serves as the reference line.

In the proposed model, the jamming loop 1 is fixed and the jamming loop 2 is rotatable. The DoA information of monopulse radar is obtained by the early warning system. Based on this information, the angle between two jamming loops are adjusted to achieve the maximum angle deception effect.

The symbol parameters in the model are described as follows:

The distance between the radar antennas is d_r; the distance between the radar antenna center and the jamming system center is r ; the half angle from the radar center to the antenna 1 and the antenna 3 is θ_{e1}; the half angle from the radar center to the antenna 2 and the antenna 4 is θ_{e2}; the baseline length of the jamming loop 1 is l, the baseline length of the jamming loop 2 is $kl(k \leq 1)$; the angle between two jamming loops is θ, $\theta \in [-\pi/2, \pi/2]$; the angle between the jamming loop 1 and the baseline is θ_c. For convenience, it is assumed that $\theta_c \in [-\pi/2, \pi/2]$ (the modulation direction of the jamming loop 1, whose value of θ_c is within the second and third quadrant, needs to be changed); the indication angle of the monopulse radar is θ_i.

The radar indication angle of the two simultaneously operated jamming loops is deduced as below.

As shown in Fig. 2, the angles θ_{e1} and θ_{e2} are given by

$$\tan\theta_{e1} = \frac{l\cos(\theta_c)/2}{r \pm l\sin(\theta_c)/2} \approx \frac{l\cos(\theta_c)}{2r} \quad (1)$$

$$\tan\theta_{e2} = \frac{kl\cos(\theta-\theta_c)/2}{r \pm l\sin(\theta-\theta_c)/2} \approx \frac{kl\cos(\theta-\theta_c)}{2r}. \quad (2)$$

Considering $r \gg l$, θ_{e1} and θ_{e2} can be written as $\theta_{e1} \approx l\cos(\theta_c)/2r$, $\theta_{e2} \approx kl\cos(\theta-\theta_c)/2r$.

The antenna gain of the monopulse radar in the sum and difference channels in the direction of the four jamming antennas is given by

$$S_{1,3} = P_r(\theta_r \pm \theta_{e1})\cos[\frac{1}{2}\beta d_r\sin(\theta_r \pm \theta_{e1})] \quad (3)$$

$$S_{2,4} = P_r(\theta_r \pm \theta_{e2})\cos[\frac{1}{2}\beta d_r\sin(\theta_r \pm \theta_{e2})] \quad (4)$$

$$D_{1,3} = jP_r(\theta_r \pm \theta_{e1})\sin[\frac{1}{2}\beta d_r\sin(\theta_r \pm \theta_{e1})] \quad (5)$$

$$D_{2,4} = jP_r(\theta_r \pm \theta_{e2})\sin[\frac{1}{2}\beta d_r\sin(\theta_r \pm \theta_{e2})]. \quad (6)$$

Where S_i and D_i represent the gain of the sum channel and the difference channel in each jamming antenna's direction, respectively;$P_r(\cdot)$ represents the gain of the radar antenna; and $\beta = 2\pi/\lambda$ is the Boltzmann constant.

Because the two semi angles are small, in order to facilitate the analysis of the formula, some terms of the formula are approximately simplified as follows:

$$\text{if}: \quad R_1 = \frac{1}{2}\beta d_r\sin\theta_r \quad R_2 = \frac{1}{2}\beta d_r\theta_{e1}\cos\theta_r$$
$$R_3 = \frac{1}{2}\beta d_r\theta_{e2}\cos\theta_r$$

The sum and difference channel gains can be written asčž

$$S_{1,3} = P_r(\theta_r \pm \theta_{e1})\cos(R_1 \pm R_2) \quad (7)$$

$$S_{2,4} = P_r(\theta_r \pm \theta_{e2})\cos(R_1 \pm R_3) \quad (8)$$

$$D_{1,3} = jP_r(\theta_r \pm \theta_{e1})\sin(R_1 \pm R_2) \quad (9)$$

$$D_{2,4} = jP_r(\theta_r \pm \theta_{e2})\sin(R_1 \pm R_3) \quad (10)$$

Considering the different modulation directions of two jamming loops may reduce the jamming signal power in the difference channel of the monopulse radar which leads to weakness of angle deception effect. It is assumed that the signal modulation direction of the jamming loop 1 is from antenna 1 to antenna 3. The influence of modulation direction of the jamming loop 2 on the jamming effect is derived as below.

(1) When the signal modulation direction of the jamming loop 2 is from antenna 2 to antenna 4, the signals received by the sum and difference channels of the monopulse radar are written as

$$\begin{aligned} S_J = {} & S_3P_c(\theta_c-\theta_{e1})S_1P_c(\theta_c+\theta_{e1}) \\ & +a_1e^{j\phi_1}S_1P_c(\theta_c+\theta_{e1})S_3P_c(\theta_c-\theta_{e1}) \\ & +S_4P_c(\theta_c-\theta_{e2})S_2P_c(\theta_c+\theta_{e2}) \\ & +a_2e^{j\phi_2}S_2P_c(\theta_c+\theta_{e2})S_4P_c(\theta_c-\theta_{e2}) \end{aligned} \quad (11)$$

$$\begin{aligned} D_J = {} & S_3P_c(\theta_c-\theta_{e1})D_1P_c(\theta_c+\theta_{e1}) \\ & +a_1e^{j\phi_1}S_1P_c(\theta_c+\theta_{e1})D_3P_c(\theta_c-\theta_{e1}) \\ & +S_4P_c(\theta_c-\theta_{e2})D_2P_c(\theta_c+\theta_{e2}) \\ & +a_2e^{j\phi_2}S_2P_c(\theta_c+\theta_{e2})D_4P_c(\theta_c-\theta_{e2}). \end{aligned} \quad (12)$$

where S_J and D_J represent the signals received by the sum and difference channels of the monopulse radar when two jamming loops working at the same time; a_1, ϕ_1, a_2 and ϕ_2 represent the amplitude ratio and the phase difference caused by the jammer modulation of the two jamming loops signals, respectively;$P_c(\cdot)$ is the gain of the jammer antenna in the direction of radar.

In formula (11) and (12), θ_{e1} and θ_{e2} are very small, the following formulas can be simplified as

$$P_r^2(\theta r \pm \theta_{e1}) \approx P_r^2(\theta_r)$$
$$P_c(\theta_c-\theta_{e1})P_c(\theta_c+\theta_{e1}) \approx P_c^2(\theta_c)$$
$$P_c(\theta_c-\theta_{e2})P_c(\theta_c+\theta_{e2}) \approx P_c^2(\theta_c)$$

The monopulse error can be obtained by dividing the difference channel return in (12), by the sum channel return in (11) and taking the image part of the result giving in (13), as shown at the bottom of this page, where $\Im(\cdot)$ and $\Re(\cdot)$ respectively represent the real part and the imaginary part of the formula; and $T_i = a_ie^{j\phi i}$ is determined by the modulation parameters of the jamming loops.

(2) When the signal modulation direction of the jamming loop 2 is from antenna 4 to antenna 2, the signals received by the sum and difference channels of the monopulse radar are written as

$$\begin{aligned} S'_J = {} & S_3P_c(\theta_c-\theta_{e1})S_1P_c(\theta_c+\theta_{e1}) \\ & +a_1e^{j\phi_1}S_1P_c(\theta_c+\theta_{e1})S_3P_c(\theta_c-\theta_{e1}) \\ & +a_2e^{j\phi_2}S_4P_c(\theta_c+\theta_{e2})S_2P_c(\theta_c-\theta_{e2}) \\ & +S_2P_c(\theta_c-\theta_{e2})S_4P_c(\theta_c+\theta_{e2}) \end{aligned} \quad (14)$$

$$\begin{aligned} D'_J = {} & S_3P_c(\theta_c-\theta_{e1})D_1P_c(\theta_c+\theta_{e1}) \\ & +a_1e^{j\phi_1}S_1P_c(\theta_c+\theta_{e1})D_3P_c(\theta_c-\theta_{e1}) \\ & +a_2e^{j\phi_2}S_4P_c(\theta_c+\theta_{e2})D_2P_c(\theta_c-\theta_{e2}) \\ & +S_2P_c(\theta_c-\theta_{e2})D_4P_c(\theta_c+\theta_{e2}). \end{aligned} \quad (15)$$

$$M_J = \Im\{\frac{D_J}{S_J}\} = \Re\{\frac{(2+T_1+T_2)\sin(2R_1)+(1-T_1)\sin(2R_2)-(1-T_2)\sin(2R_3)}{(2+T_1+T_2)\cos(2R_1)+(1+T_1)\cos(2R_2)+(1+T_2)\cos(2R_3)}\}. \quad (13)$$

$$M'_J = \Im\{\frac{D'_J}{S'_J}\} = \Re\{\frac{(2+T_1+T_2)\sin(2R_1)+(1-T_1)\sin(2R_2)-(1-T_2)\sin(2R_3)}{(2+T_1+T_2)\cos(2R_1)+(1+T_1)\cos(2R_2)+(1+T_2)\cos(2R_3)}\}. \quad (16)$$

TABLE 1. Simulation parameters.

Parameters	VALUE
the frequency of radar signal	10 GHz
d_r	2.54 times of wavelength
r	2km
θ_c	[-90°,90°]
θ_r	10°
θ	[-90°,90°]

Then the monopulse error can also be written in (16), as shown at the bottom of previous page.

Finally, the relationship between the radar indication angle and the monopulse error is given by

$$\theta_i=\arcsin\{\frac{2}{\beta d_r}\arctan(\mathrm{Max}\{M_J, M_J'\})\}. \tag{17}$$

The radar indication angle reflects the jamming effect of cross-eye jamming system on monopulse radar. In the proposed model, the jamming system is on the target platform. It can be found in Fig.2 that the radar will point to the target platform when $\theta_i \in [\theta_r-\theta_e, \theta_r+\theta_e]$. Assuming that the false target located above the target platform, the radar indication angle needs to be met the standard of $\theta_i > \theta_r + \theta_e$.

III. SIMULATION AND ANALYSIS

In this section, the simulation analysis of the four-element retrodirective cross-eye model based on DoA is carried out. The influence of the antenna distribution and the modulation parameter selection on the jamming performance of the model proposed is studied. The simulation parameters are given in Table 1.

A. JAMMING ANTENNA DISTRIBUTION

In order to analyze the influence of the modulation direction of the jamming loop 2 on the jamming performance, the relationship between the radar indicator angle and the modulation direction of the jamming loop 2 is observed by using different modulation parameters and different θ_c, respectively ($a_1 = 0.9, 0.7, 0.5, 0.3, \varphi_1 = 175°, 165°, 155°, 145° a_2 = 0.8, 0.6, 0.4, 0.2, \varphi_1 = 170°, 160°, 150°, 140°$). The results are as follows.

As shown in Fig. 3, the left side of the dotted line in the longitudinal direction indicates that the modulation direction of the jamming loop 2 is from antenna 2 to antenna 4. The right side of the dotted line in the longitudinal direction indicates that the modulation direction is from antenna 4 to antenna 2. Fig. 3 shows that in order to get the optimum value of θ_i, the modulation direction is determined by the value of θ when the value of θ_c is fixed; and even if the modulation parameters are different, the modulation direction should be changed in the same position($|\theta-\theta_c| = \pi/2$). Based on the comprehensive analysis of the results, we are glad to find that: if $|\theta-\theta_c| > \pi/2$, the modulation direction of the jamming loop 2 is from antenna 4 to antenna 2; else, the modulation direction of the jamming loop 2 is from antenna 2 to antenna 4, which can make the radar indicator angle larger.

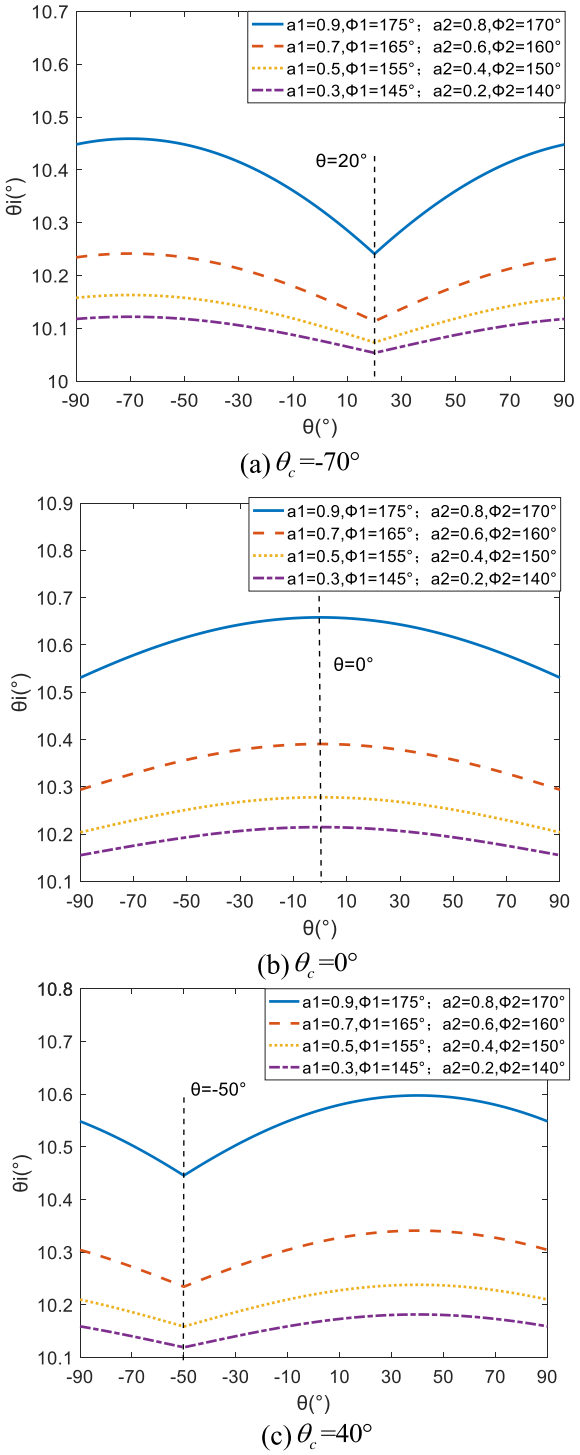

FIGURE 3. Optimum θ_i with different modulation parameters.

When the modulation parameters of the jamming loops are fixed ($a_1 = 0.8, \varphi_1 = 165° a_2 = 0.7, \varphi_2 = 150°$),

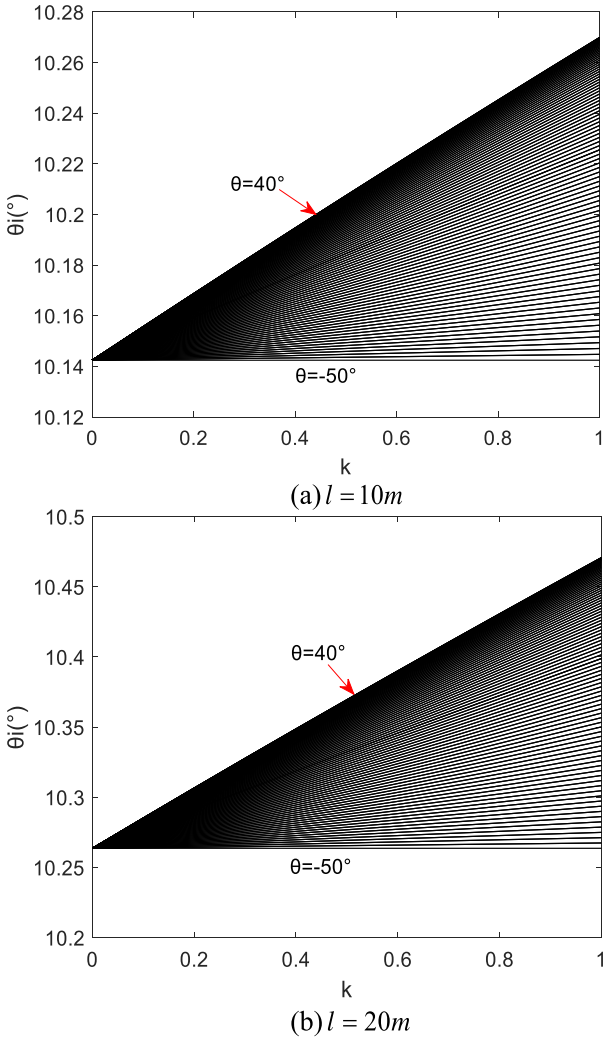

FIGURE 4. Relationship between length of jamming loops and radar indication angle.

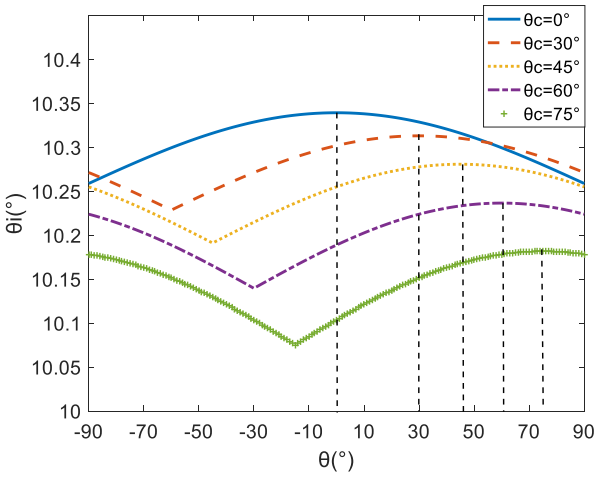

FIGURE 5. Relationship between the angle between jamming loops and radar indication angle.

the influence of value of k on the radar indication angle is compared when the length of jamming loop 1 is different, the results are shown in Fig. 4.

The results in Fig. 4 reflect the relationship between k and the radar indication angle when θ is taken different values ($\theta \in [-90°, 90°]$). It can be found that with the increase of the length of the jamming loop 1, the radar indication angle becomes larger, the deception effect on the monopulse radar will be better at the same time. It can be concluded that the radar indication angle will become larger with the increasing of k even if θ is different.

In order to analyze the influence of θ on the jamming effect, the relationship between the radar indicator angle and the angle of jamming loop is obtained when using different values of θ_c, the results are shown in Fig. 5.

As shown in Fig.5, when θ_c is taken different values, the curves represent the relationship between θ_i and θ, the dotted line in the longitudinal direction indicates the value of θ when θ_i take the peak value. And it can be concluded when $\theta = \theta_c$, the radar indicator angle is the largest, which indicates the best jamming performance. It also provides a certain optimization basis for the distribution of jamming system.

The jamming model proposed in this paper can be optimized based on the analysis results in front. The length of jamming loops is generally determined by the size of the target platform in application, and the angle between two jamming loops can be adjusted to meet the condition of $\theta = \theta_c$ by rotating the jamming loop 2 based on the DoA information obtained by the early warning system. And $|\theta - \theta_c| = 0° < \pi/2$, the modulation direction of jamming loop 2 is from antenna 2 to antenna 4.

B. COMPARATIVE ANALYSIS

After optimizing the jamming model proposed in Section A, the influence of the modulation parameters on the jamming effect is analyzed in this section, and compared with the traditional retrodirective cross-eye jamming model and the orthogonal four-element jamming model in reference [19].

As mentioned in Section 2, in order to make the radar Los point to the position outside the target platform, it is necessary to meet the condition of $\theta_i > \theta_r + \theta_e$. If $l = 15m$, $\theta_i > 10.004°$. The relationship between the modulation parameters of the two jamming loops and the radar indication angle is analyzed as follows.

As shown in Fig. 6(a), the curve shows the relationship between the modulation parameters of jamming loop 2 and the contour of $\theta_i = 10.004°$, when the modulation parameters of the jamming loop 1 are fixed. The area below the curve indicates the corresponding value when the condition of $\theta_i > 10.004°$ is satisfied. It can be found that when the modulation parameters of jamming loop 1 are fixed($a_1 = 0.8$, $\phi_1 = 160°$), the phase difference of jamming loop 2 can take any value if the amplitude ratio meet the condition of $a_2 < 0.98$, it means that the value space of the phase difference is large. As shown in Fig. 6(b), the curve shows

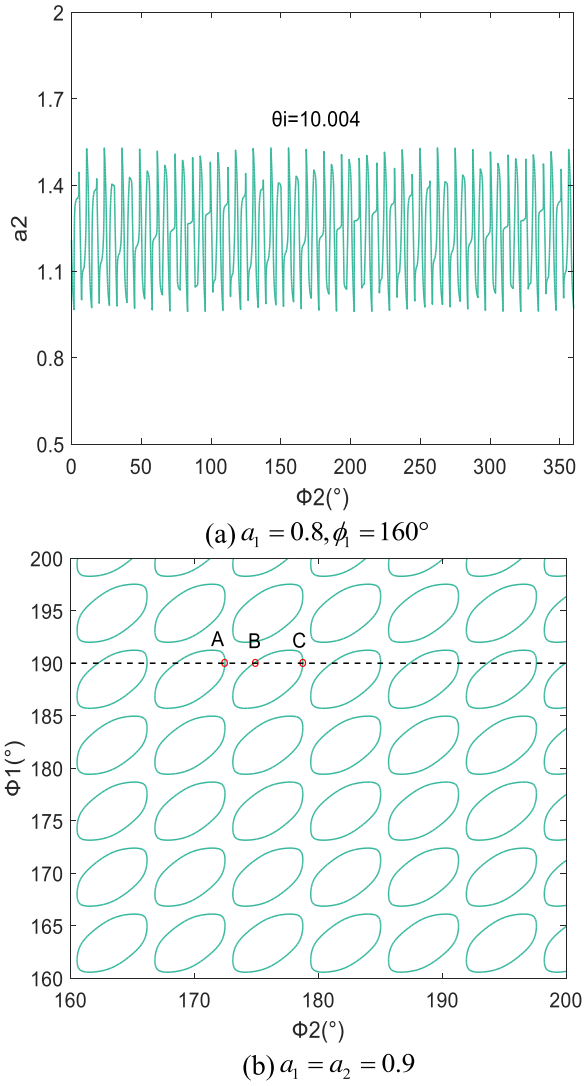

FIGURE 6. Relationship between modulation parameters and radar indication angle.

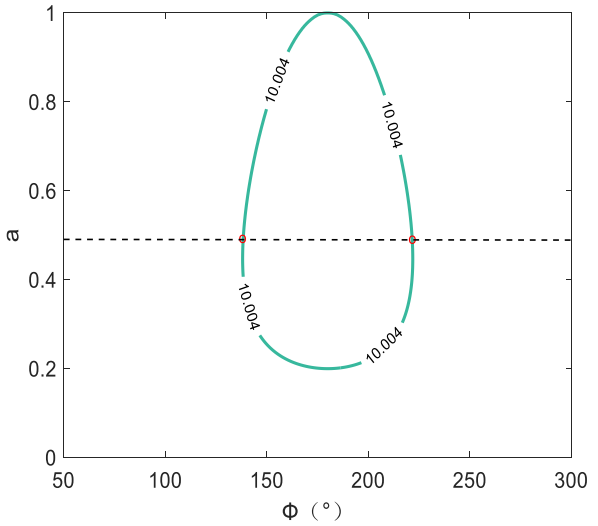

FIGURE 7. Relationship between the modulation parameters and the radar indication angle of the traditional retrodirective cross-eye jamming model.

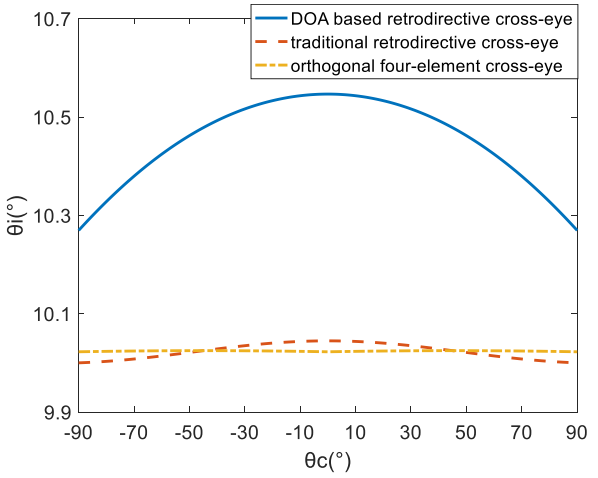

FIGURE 8. Radar indication angle comparison of different cross-eye jamming models.

the relationship between the phase difference of two jamming loops and the contour of $\theta_i = 10.004°$ when the amplitude ratio of two jamming loops are fixed ($a_1 = a_2 = 0.9$). The area outside the circle indicates the corresponding value when the condition of $\theta_i > 10.004°$ is met. The dotted line in the Fig.6(b) indicates that $\phi_1 = 190°$, the values corresponding to the intersection points A, B and C are $\phi_2 = 172.5°\phi_2 = 174.9°\phi_1 = 178.7°$ respectively. It can be estimated that the value space of ϕ_2 that meets the condition $360° \times \frac{174.9-172.5}{178.7-172.5} \approx 139.4°$.

As shown in Fig..7, the curve shows the relationship between the modulation parameters of the traditional retrodirective cross-eye jamming model, and the contour of $\theta_i = 10.004°$. The area inside the circle indicates the corresponding value when the condition of $\theta_i > 10.004°$ is met. The dotted line in the figure shows when the amplitude ratio is $a = 0.44$, the maximum value space of the phase difference can be obtained as $221.6° - 138.4° = 83.2°$, which is far less than that in Fig. 6(b).

The jamming effect of the model proposed in this paper on the monopulse radar from different direction is compared with the traditional retrodirective cross-eye jamming model, and the orthogonal four-element retrodirective cross-eye jamming model under the same condition($a_1 = a2 = 0.9$, $\phi_1 = \phi_2 = 170°$).

As shown in Fig. 8, the jamming effect of the jamming model proposed in this paper is better than the other two jamming models under the same condition.

IV. CONCLUSION

In this paper, the four-element retrodirective cross-eye jamming model based on DoA is established. The influence of distribution and modulation parameters of jamming loops on

the jamming effect is studied. The following conclusions can be obtained through the simulation results:

(1) For different platforms, the longer the jamming loops length, the better the jamming effect of the interference system;

(2) After obtaining DoA information, the jamming effect of the proposed jamming model is better by rotating the jamming loop 2 to meet the condition of $\theta = \theta_c$.

(3) On the premise of getting the same interference effect, the proposed jamming model is better than the traditional two-element jamming model in the value space of the modulation parameter. It is also better than the traditional two-element jamming model and the orthogonal four-element jamming model in the interference effect when taking the same modulation parameters.

The research conclusion provides a guidance for the engineering design.

REFERENCES

[1] S. M. Sheerman and D. K. Barton, *Monopulse Principles and Techniques*. Norwood, MA, USA: Artech House, 2011.
[2] S.-H. Lee, S.-J. Lee, I.-O. Choi, and K.-T. Kim, "ICA-based phase-comparison monopulse technique for accurate angle estimation of multiple targets," *IET Radar, Sonar Navigat.*, vol. 12, no. 3, pp. 323–331, Mar. 2018.
[3] G. Q. Zhao, *Principle of Radar Countermeasure*. Xi'an, China: Xidian Univ. Press, 1999.
[4] (2011). *EW: Counter-Missile Technologies*. [Online]. Available: http://www.skyindustries.com
[5] K. Y. Guo, T. Y. Niu, and X. Q. Sheng, "Influence of multiple scattering centers with various attributes on radar angular measurements," *J. Electron. Inf. Technol.*, vol. 9, pp. 2238–2244, Jan. 2017.
[6] T. P. Liu, X. Z. Wei, and Z. Liu, "Overview of cross-eye jamming research," *J. Radars*, vol. 8, no. 1, pp. 140–153, 2019.
[7] D. C. Schleher, *Electronic Warfare in The Information Age*. Norwood, MA, USA: Artech House, 1999.
[8] B. Petersson, "Error estimation in retrodirective channel implementation," in *Proc. IEEE Int. Conf. Microw., Antennas, Commun. Electron. Syst. (COMCAS)*, Tel-Aviv, Israel, Dec. 2017, pp. 120–125.
[9] G. Y. Ge, *Research on Application Technology of Retrodirective Array*. Nanjing, China: Nanjing University of Science & Technology, 2009.
[10] W. P. duPlessis, J. W. Odendaal, and J. Joubert, "Tolerance analysis of cross-eye jamming systems," *IEEE Trans. Aerosp. Electron. Syst.*, vol. 47, no. 1, pp. 740–745, Jan. 2011.
[11] W. P. duPlessis, J. W. Odendaal, and J. Joubert, "Experimental simulation of retrodirective cross-eye jamming," *IEEE Trans. Aerosp. Electron. Syst.*, vol. 47, no. 1, pp. 734–740, Jan. 2011.
[12] P. W. P. Du, "Cross-eye gain in multi-loop retrodirective cross-eye jamming," IEEE Transactions on Aerospace and Electronic Systems, 2016, vol. 52, no. 2, pp. 875–882.
[13] W. P. du Plessis, "Analysis of path-length effects in multiloop cross-eye jamming," *IEEE Trans. Aerosp. Electron. Syst.*, vol. 53, no. 5, pp. 2266–2276, Oct. 2017.
[14] Q. Y. Liu and L. Ma, "Characteristic analysis of cross-eye jamming of monopulse radar signals," *Aerosp. Electron. Warfare*, vol. 32, no. 1, pp. 59–61, 2016.
[15] L. Zhou, J. Meng, and H. Wu, "Interference modeling of two point source retrodirective cross-eye considering target echo," *J. Electron. Inf. Technol.*, vol. 41, no. 4, pp. 816–821, 2019.
[16] S. Y. Liu, C. X. Dong, and Z. T. Zhu, "Tolerance analysis of rotating cross-eye jamming based on angle factor specific boundary value," *J. Electron. Inf. Technol.*, vol. 38, no. 4, pp. 906–912, 2016.
[17] S.-Y. Liu, C.-X. Dong, J. Xu, G.-Q. Zhao, and Y.-T. Zhu, "Analysis of rotating cross-eye jamming," *IEEE Antennas Wireless Propag. Lett.*, vol. 14, pp. 939–942, 2015.
[18] T. Liu, D. Liao, X. Wei, and L. Li, "Performance analysis of multiple-element retrodirective cross-eye jamming based on linear array," *IEEE Trans. Aerosp. Electron. Syst.*, vol. 51, no. 3, pp. 1867–1876, Jul. 2015.
[19] T. Liu, Z. Liu, D. Liao, and X. Wei, "Platform skin return and multiple-element linear retrodirective cross-eye jamming," *IEEE Trans. Aerosp. Electron. Syst.*, vol. 52, no. 2, pp. 821–835, Apr. 2016.
[20] D. G. Yang, B. G. Ling, and D. J. Zhao, "Cross-eye gain distribution of multiple-element retrodirective cross-eye jamming," *J. Syst. Eng. Electron.*, vol. 29, no. 6, pp. 1170–1179, 2018.
[21] W. Liu, J. Meng, and L. Zhou, "Interference modeling of rectangular array retrodirective cross-eye jamming method," *J. Syst. Eng. Electron.*, vol. 41, no. 11, pp. 2453–2459, 2019.
[22] F.-G. Yan, S. Liu, J. Wang, M. Jin, and Y. Shen, "Fast DOA estimation using co-prime array," *Electron. Lett.*, vol. 54, no. 7, pp. 409–410, Apr. 2018.
[23] J. Z. Ma, L. F. Shi, and S. P. Xiao, "Mitigation of cross-eye jamming using a dual-polarization array," *J. Syst. Eng. Electron.*, vol. 29, no. 3, pp. 491–498, 2018.
[24] D. E. N. Davies, "Some properties of van atta arrays and the use of 2-way amplification in the delay paths," *Proc. Inst. Electr. Eng.*, vol. 110, no. 3, p. 507, 1963.
[25] A. Abdalla, M. G. S. Ahmed, Y. Zhao, Y. Xiong, and B. Tang, "Deceptive jamming suppression in multistatic radar based on coherent clustering," *J. Syst. Eng. Electron.*, vol. 29, no. 2, pp. 269–277, Apr. 2018.

WEI LIU was born in Hubei, China, in 1991. He received the B.S. and M.S. degrees in cyberspace security from the Naval University of Engineering, Wuhan, China, in 2013 and 2016, respectively, where he is currently pursuing the Ph.D. degree in electrical engineering.

His research interest includes the jamming effect evaluation of radar and signal interference in complex electromagnetic environment.

JIN MENG was born in Henan, China, in 1977. He received the B.S. degree in electrical engineering from the Chongqing College of Communication, Chongqing, China, in 1999, and the M.S. and Ph.D. degrees in electrical engineering from the Naval University of Engineering, Wuhan, China, in 2002 and 2006, respectively.

In 2006, he joined the Research Institute of Power Electronic Technology, Naval University of Engineering, as a Lecturer, where he has been a Professor in electrical engineering, since 2011. From October 2011 to September 2012, he worked as a Visiting Scholar with the George Green Institute for Electromagnetics Research, University of Nottingham. Since 2017, he has also been with the Specialized Electrical Research Institute of Science and Technology, Naval University of Engineering, where he currently the Head of the EMC Team. He is the author of two books, more than 150 articles, and more than 40 inventions. His research interests include electromagnetic compatibility (EMC) prediction both in power conversions and communication systems, novel EMI reduction techniques for radiated and conducted EMI, and compact high power microwave.

LIANG ZHOU was born in Henan, China, in 1989. He received the B.S. degree in radar engineering, the M.S. degree in antenna engineering, and the Ph.D. degree in equipment support engineering from the Naval University of Engineering, Wuhan, in 2011, 2013, and 2017, respectively.

He is currently an Assistant Researcher with the Naval University of engineering. His research interests include radar countermeasures and equipment support resource planning.